Single parameter post-processing method for image deblurring

Andrey Krylov, and Andrey Nasonov and Yakov Pchelintsev
Faculty of Computational Mathematics and Cybernetics,
Lomonosov Moscow State University
e-mail: kryl@cs.msu.ru, nasonov@cs.msu.ru

***Abstract*—Numerous algorithms exist for the problem of deconvolution of blurred images. But due to ill-posed nature of deconvolution, many images still remain blurry after deblurring. An edge sharpening algorithm is proposed in the paper to further improve the quality of blurry images in edge areas. The method is based on pixel grid warping, its main idea is to move pixels in the direction of the nearest image edges. Warping allows to make edges sharper while keeping textured areas almost intact. Experimental analysis for different optical blur models is performed to optimize the parameters of the proposed method and to show its effectiveness.**

***Index Terms*—Edge sharpening, Image deblurring, Grid warping, Optical blur**

I. INTRODUCTION

Image deblurring is a challenging ill-posed problem of finding a sharp image I_0 from given blurred image I_B using the blur model

$$I_B = I_0 * H + n$$

where H is the blur kernel and n is additive noise. If blur kernel H and noise n are known with sufficient precision, the deconvolution problem can be effectively solved by regularization-based algorithms [1].

Unfortunately in practice there is usually very little information about H and n, and the blur kernel is to be estimated. There are some fairly powerful techniques for blind image deblurring [2], [3]. Non-uniformity of image blur, noise and blur kernel estimation errors may significantly degrade the result. It is not easy to find optimal parameters for a compromise between smooth result with blurry edges and sharp result with artifacts like ringing or noise amplification when blur kernel is estimated with errors.

The aim of the paper is to develop a post-processing method for enhancement of the results of existing image deblurring algorithms. This algorithm should be stable to noise and errors in blur kernel estimation.

In this paper, we present an image sharpening method that performs an enhancement of a blurred image in the neighborhood of image edges. The idea is to transform the neighborhood of the blurred edge so that the neighboring pixels move closer to the edge, and then resample the image from the warped grid to the original uniform grid.

The warping approach is related to the morphology-based sharpening [4] and shock filters [5], [6], [7]. But these methods make the image appear piecewise constant which is effective mostly for cartoon-like images. The proposed method is applied to edges locally so the textures are preserved a priori. Also warping compresses the edge neighborhood at fixed rate and does not make the image piecewise constant.

The warping approach for image enhancement was introduced in [8]. The warping of the grid in that work is performed according to the solution of a differential equation derived from the warping process constraints. The solution of the equation is used to move the edge neighborhood closer to the edge, and the areas between edges are stretched. The method has several parameters, and the choice of optimal values for the best result is not easy. Due to the global nature of the method the resulting shapes of the edges are often distorted. In [9] warping is computed directly using the values of left and right derivatives. In both methods [8] and [9] the pixel shifts are proportional to the gradient values. It results in oversharpening of already sharp and high contrast edges and insufficient sharpening of blurry and low contrast edges. Both methods also introduce small local changes in the direction of edges and produce aliasing effect due to calculation of horizontal and vertical warping components separately.

Application of grid warping method for the enhancement of image deblurring methods was considered in [10], [11]. Nevertheless, they used the assumptions of the Gaussian based grid displacement and Gaussian blur. In this work, we improve their results by considering different blur kernels that correspond to real optic blur and suggesting more effective single-parameter displacement function.

II. OPTICAL BLUR

Optical aberration is a result of inaccuracy of light convergence in optical systems that usually leads to image blur. Different models were created to model this effect. The Seidel aberration model is one of them [12]. It consists of five kinds of optical aberrations, each having its own effect [13], [14]: spherical aberration, astigmatism, defocus blur, radial distortion and coma.

In our paper we consider three types of blur that are typical for photographic images:

1. Gaussian blur that approximates spherical aberrations. It is represented by a convolution with the Gaussian filter

$$G_\sigma(x, y) = \frac{1}{2\pi\sigma^2} \exp\left(-\frac{x^2 + y^2}{2\sigma^2}\right)$$

978-1-5386-1842-4/17/$31.00

2. Circular blur

$$C_r(x,y) = \begin{cases} 1, & x^2+y^2 \le r^2, \\ 0, & \text{otherwise}. \end{cases}$$

3. Ring blur

$$R_r(x,y) = \begin{cases} 0.25, & x^2+y^2 \le 0.75r^2, \\ 1, & 0.75r^2 < x^2+y^2 \le r^2, \\ 0, & \text{otherwise}. \end{cases}$$

The last two blur types correspond to out-of-focus blur. It appears at the areas which are in front of or behind the camera focal plane. It may be the result of such lens and camera issues as front-focus and back-focus, when the camera cannot set the focus plane properly. Also out-of-focus blur is used intentionally to create an effect called bokeh, an artistic technique in photography. In this case the blur kernel has a shape of a circle with sharp edges.

The examples of real out-of-focus blur are shown in Fig. 1. The kernels of modeled blur are shown in Fig. 2.

The results of this blur type is seen in the Figure 1.

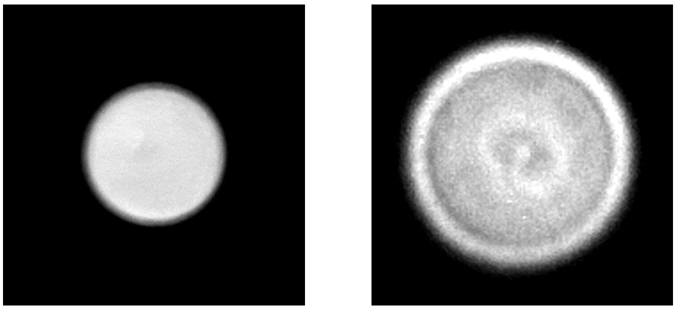

(a) Object is in front of the focus plane (b) Object is behind the focus plane

Fig. 1: Examples of real out-of-focus blur.

III. Grid warping

In this section we describe the idea of edge enhancement using pixel grid transformation.

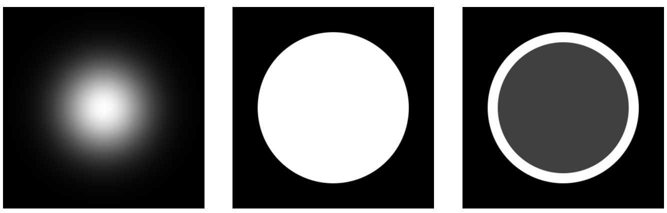

(a) Gaussian kernel (b) Circular kernel (c) Ring kernel

Fig. 2: Blur kernels used in the paper.

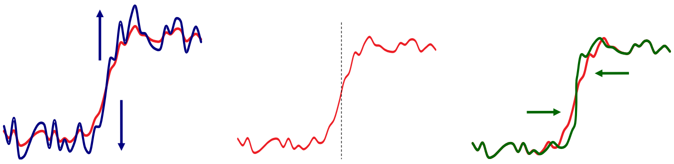

(a) Typical image enhancement approach (b) Edge profile (c) Warping approach: pixels are shifted

Fig. 3: The idea of edge sharpening by grid warping.

A. *One-dimensional edge sharpening*

The profile of a blurred edge is more gradual compared to a sharp edge profile. So in order to make the edge sharper its transient width should be decreased (see Fig. 3).

For any edge $g(x)$ centered at $x = 0$ its sharper version $h(x)$ can be obtained shifting the pixels from the neighborhood of the edge towards its center. The *displacement function* $d(x)$ describes the shift of a pixel with coordinate x to a new coordinate $x + d(x)$ [11]: $h(x + d(x)) = g(x)$.

The warped grid must remain monotonic (i.e. for any $x_1 < x_2$ new coordinates must be $x_1 + d(x_1) \le x_2 + d(x_2)$), so the displacement function should match the following constraint:

$$d'(x) \ge -1. \tag{1}$$

Another constraint localizes the area of warping effect far from the edge center:

$$d(x) \to 0, \qquad |x| \to \infty.$$

The displacement function $d(x)$ greatly influences the result of the edge warping. On the one hand, the edge slope should become steeper. On the other hand, the area near the edge should not be stretched over some predefined limit to avoid wide gaps between adjacent pixels in the discrete case. The choice of the displacement function is discussed in the following sections.

B. *Grid warping for 2D images*

The papers [10], [11] describe how grid warping for edge sharpening is applied for 2D images.

1) Single-edge algorithm: The simplest algorithm is finding the nearest edge for every pixel and apply the one-dimensional algorithm using that edge (see Fig. 4). It consists of the following steps:

1. Estimate the blur level (the average standard deviation of Gaussian filter) for the edges.
2. For all pixels in the neighborhood of the edge compute the distance x to the nearest edge point.
3. Calculate the displacement value $d(x)$ and perform pixel shift towards the edge.
4. Interpolate the image from the warped grid to the old uniform grid.

The edge map at the input of the algorithm has a great influence on the result of grid warping as only detected edges will be sharpened. We use the result of Canny edge detection [15] as the input of the algorithm. The result of image warping

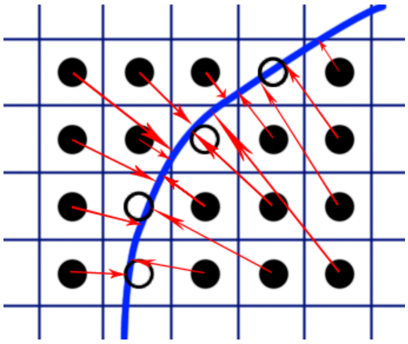

Fig. 4: Displacements for two-dimensional grid warping. Thick blue line represents the exact edge location, white circles represent edge pixels, black circles represent pixels from the edge neighborhood.

is highly dependent on the parameters of the Canny method (σ and high threshold T_{high}).

2) Multi-edge algorithm: Multi-edge algorithm performs grid warping towards all edges in the neighborhood of the processed pixel using weighted averaging of individual warping vectors for each edge pixel. The weights are proportional to the distance to edge pixels, to gradient magnitude in edge pixels and to angle between gradient direction and the line connecting edge pixels and processed pixel:

$$\vec{d}(P) = \frac{\sum_{Q\in E(P)} w(P,Q)\vec{n}(Q)d((\vec{n}(Q), P-Q))}{\sum_{Q\in E(P)} w(P,Q)},$$

where $\vec{n}(Q) = \frac{\vec{g}(Q)}{|\vec{g}(Q)|}$ is the unit vector corresponding to edge profile (gradient) direction, $(\vec{n}(Q), P-Q)$ is the projection of the vector $\overrightarrow{PQ}$ onto the one-dimensional edge profile, $E(P)$ is the set of edge pixels Q in the neighbourhood of processed pixel P and $w(P,Q)$ is weight coefficient. The size of the neighborhood is chosen in accordance to the support of the displacement function $d(x)$.

The weight coefficient $w(P,Q)$ is defined as

$$w(P,Q) = |\vec{g}(Q)| \exp\left(-\frac{|P-Q|^2 - (P-Q,\vec{n}(Q))^2}{2\sigma_w^2}\right),$$

where the value $|P-Q|^2 - (P-Q,\vec{n}(Q))^2$ is the squared rejection of the vector $P-Q$ onto edge profile direction. The value σ_w is chosen proportional to the blur level. For Gaussian blur with parameter σ, we use $\sigma_w = 2.5\sigma$.

3) Interpolation: The idea of interpolation from the warped grid to the uniform grid is as follows: the intensity of the image at pixel P is computed as a weighted sum of intensities of all points on the warped grid in the neighborhood of the pixel (see Fig. 5c): for a given radius ρ and all neighboring points $N(P) = \{Q : |Q-P| \le \rho\}$ the intensity of a warped image I_w at P is computed as

$$I_w(P) = \frac{\sum_{Q\in N(P)} \frac{1}{|P-Q|} I(x_k,y_k)}{\sum_{Q\in N(P)} \frac{1}{|P-Q|}}.$$

We use the interpolation radius $\rho = 1.5$. Its size is determined by the maximal distance between pixels after grid warping. The interpolation step introduces small blur effect but its influence on the sharpness improvement is very small.

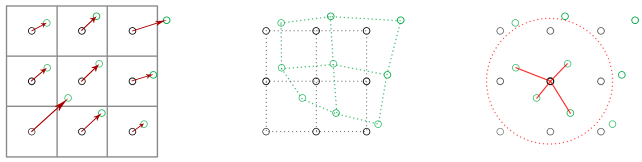

(a) displacements (b) warped grid (c) interpolation

Fig. 5: Interpolation after grid warping

IV. Displacement function

We use the assumption that displacement functions should be proportional to the blur level within the same blur type. Let $d_0(x)$ be the displacement function corresponding to unit blur. Then the displacement function for the same blur type with blur parameter t should look as follows:

$$d(x) = t d_0(\frac{x}{t}). \tag{2}$$

A. Models

Two models have been considered for the choice of the displacement function.

1. The difference of Gaussian functions:

$$d_1(x) = s\sqrt{\pi}\left(\operatorname{erf}\left(\frac{x}{2s}\right) - \operatorname{erf}\left(\frac{x}{s}\right)\right),$$

where

$$\operatorname{erf}(x) = \frac{2}{\sqrt{\pi}}\int_0^x e^{-t^2}dt.$$

This type of displacement function was applied to images blurred with Gaussian blur [10], [11]. For unit Gaussian blur the parameter $s = 1$ is used. For circular and ring blur parameter s is to be estimated experimentally. One of the drawbacks of this model is insufficient increase of edge sharpness. Therefore, in this work, we suggest another model that gives sharper edges.

2. Piecewise linear function:

$$d_2'(x)[a,b,c] = \begin{cases} \frac{c}{a}x, & |x| \le a, \\ c\frac{b-|x|}{b-a}\operatorname{sign} x, & a < |x| \le b, \\ 0, & |x| > b. \end{cases}$$

The parameters a, b and c define the width of densification and rarefication areas and the steepness of the displacement function. The strongest warping effect that meets the condition (1) is achieved with $c = -a$. Therefore, we use the displacement function with two parameters:

$$d_2(x)[a,b] =$$

$$= d_2'(x)[a,b,-a] = \begin{cases} -x, & |x| \le a, \\ -a\frac{b-|x|}{b-a}\operatorname{sign} x, & a < |x| \le b, \\ 0, & |x| > b. \end{cases}$$

B. Finding optimal parameters of displacement functions

We have found optimal parameters for each analyzed displacement function for each blur type. Due to the assumption (2) there is no need to estimate the displacement function parameters for each blur level. Instead we estimate the parameters corresponding to unit blur.

1) Image set: Test images were generated using 24 natural images from TID2013 database [16]. Each reference image was convolved with the mentioned above blur kernels with different blur levels. The radius r of circular and ring blur was within the range $[1.5, 5]$ with the step 0.5. The parameter σ of Gaussian blur was within the range $[0.75, 2.5]$ with the step 0.25.

2) Parameter optimization: The optimal parameters for each blur type were obtained by error minimization:

$$\sum_k \|u_k - v_k\|_2 \to \min,$$

where $\|\cdot\|_2$ is Euclidean norm, v_k is the result of grid warping applied to the blurred image, u_k is the corresponding ground truth image.

For solving the minimization problem for displacement functions containing multiple parameters, the Nelder-Mead algorithm was used. The number of iterations was limited to 100, and the minimal step was set to 10^{-3} of the blur parameter. The initial approximation was $a = 1, b = 1, s = 1$. With these parameters the method stopped at about the 50-th iteration because of the step size limitation. Various initial approximations were taken to achieve the global minimum.

C. Generalization

During the experiments, it was found that the parameters a and b of the function d_2 were very different. At the same time, the dependence of image quality on the parameter b was insignificant. So we decided to add the third displacement function model $d_3(x)$ with parameter b set to $\frac{3}{2}a$:

$$d_3(x)[a] = d_2(x)[a, \frac{3}{2}a] = \begin{cases} -x, & |x| \le a, \\ \frac{3a-2|x|}{a} \operatorname{sign} x, & a < |x| \le \frac{3}{2}a, \\ 0, & |x| > \frac{3}{2}a. \end{cases}$$

V. Results

A. Displacement function analysis

Table I shows the PSNR results for image sharpening by grid warping using three models d_1, d_2, d_3 for the considered blur types. It can be seen that an application of the grid warping algorithm to blurred images results in the increase of image quality with model d_2 showing the best results. Compared to the model d_2, the model d_3 has almost the same quality with unnoticeable visual difference. Gaussian-based d_1 has slightly worse quality due to insufficient edge sharpening.

Taking into account the results, the rest of the experiments in the paper are conducted with the model d_3. The obtained optimal values of the parameter a for the model d_3 are the following: for Gaussian blur $a = 1.28$, for circular blur $a = 1.12$ and for ring blur $a = 1.16$.

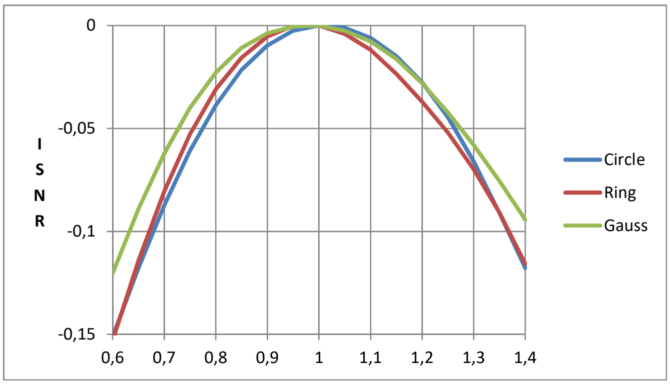

Fig. 6: The decrease of PSNR values for incorrectly estimated blur level. The ISNR — PSNR difference between blurred and warped image is about 0.3 dB

B. Stability

One of the problems of image deblurring algorithms is the strong dependence of the result on the estimation of blur kernel. We have investigated what happens to the results of the proposed algorithm when the blur parameter is estimated incorrectly. The graph in Fig. 6 shows the difference between optimal and obtained PSNR values depending on the relative error of blur estimation for the test image set.

It can be seen that blur level estimation error does not influence the stability of the proposed method. The grid warping method still improves the image even with 40% relative error.

C. Post-processing

We applied the image warping with the displacement function model d_3 as a post-processing algorithm for image deblurring and TV image enhancement algorithms. The same reference images from TID database [16] were used but the scenario was different. The images were blurred with each of three blur types (Gaussian blur, circular and ring blur) with random blur parameter in the range $[1, 5]$, then Gaussian white noise with random standard deviation in the range $[0, 10]$ was added. After that we applied existing deblurring algorithms followed by image warping using known blur level. PSNR results are shown in Table III.

Figure 7 demonstrates visual quality. It is shown that grid warping algorithm improves image quality in most edge areas (green areas in SSIM difference images). At the same time, small areas of degradation also exist (red areas in SSIM difference images). Usually, the degradation occurs when the edge becomes more sharp than in the reference image.

The execution time of image warping algorithm for 512×512 image is about a second for Intel Core i7 processor. Fast GPU implementation of the proposed algorithm is possible [19].

Blur	Gaussian blur				Circular blur				Ring blur			
param	Orig	d_1	d_2	d_3	Orig	d_1	d_2	d_3	Orig	d_1	d_2	d_3
1.5	25.543	25.773	25.842	25.842	28.351	28.483	28.561	28.555	27.300	27.468	27.608	27.621
2.0	24.335	24.587	24.660	24.660	26.657	26.853	26.923	26.929	25.508	25.735	25.870	25.869
2.5	23.571	23.842	23.908	23.908	25.290	25.535	25.612	25.614	24.355	24.621	24.755	24.741
3.0	23.008	23.276	23.335	23.335	24.623	24.869	24.930	24.929	23.843	24.104	24.207	24.197
3.5	22.578	22.841	22.894	22.894	23.998	24.256	24.310	24.307	23.276	23.546	23.634	23.627
4.0	22.220	22.478	22.527	22.527	23.577	23.827	23.873	23.870	22.903	23.165	23.239	23.234
4.5	21.922	22.182	22.228	22.228	23.208	23.461	23.499	23.498	22.568	22.832	22.895	22.889
5.0	21.658	21.912	21.959	21.959	22.896	23.141	23.175	23.174	22.286	22.543	22.599	22.591
Aver	**23.104**	**23.361**	**23.419**	**23.419**	**24.825**	**25.053**	**25.110**	**25.110**	**24.005**	**24.252**	**24.351**	**24.346**

TABLE I: PSNR values for image warping for considered blur models and displacement functions for different blur levels.

	Gaussian blur		Circular blur		Ring blur	
	Before	After	Before	After	Before	After
Blurred and noisy images	23.63	23.94	26.13	26.38	23.70	24.06
Unsharp masking	23.08	23.36	24.91	25.08	22.80	23.05
TV regularization	23.68	23.69	23.27	23.30	22.60	22.60
Low-frequency TV reg. [17]	23.65	23.89	26.42	26.56	23.07	23.30
TVMM [1]	24.95	25.08	25.85	25.92	23.01	23.07
Lucy-Richardson [18]	24.37	24.51	25.52	25.67	24.44	24.56
Wiener [18]	24.96	25.17	24.97	25.09	23.87	23.98
MatLab blind deconvolution	24.29	24.44	25.57	25.72	24.43	24.56
Average	**24.08**	**24.26**	**25.33**	**25.47**	**23.49**	**23.65**

TABLE II: Improvement of PSNR values by grid warping algorithm after different image deblurring methods for test image with added blur and noise

	Gaussian blur		Circular blur		Ring blur	
	Before	After	Before	After	Before	After
Blurred and noisy images	0.541	0.553	0.654	0.663	0.529	0.545
Unsharp masking	0.457	0.469	0.565	0.574	0.446	0.459
TV regularization	0.570	0.575	0.667	0.668	0.526	0.532
Low-frequency TV reg. [17]	0.519	0.527	0.660	0.664	0.486	0.496
TVMM [1]	0.684	0.687	0.692	0.694	0.601	0.602
Lucy-Richardson [18]	0.567	0.573	0.593	0.598	0.568	0.573
Wiener [18]	0.642	0.648	0.565	0.570	0.533	0.538
MatLab blind deconvolution	0.560	0.566	0.595	0.600	0.568	0.573
Average	**0.567**	**0.574**	**0.624**	**0.629**	**0.532**	**0.540**

TABLE III: Improvement of SSIM values by grid warping algorithm after different image deblurring methods for test image with added blur and noise

Reference image

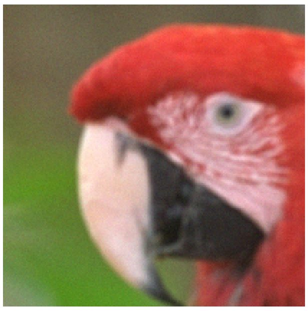

Degraded image by circular blur $r = 2.92$, noise $= 3.82$, PSNR=26.31

Wiener method [18]
PSNR=26.47

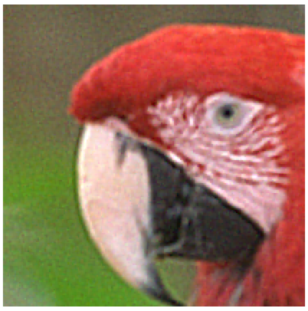

Low-frequency TV regularization [17]
PSNR=27.86

Wiener + warping
PSNR=26.61

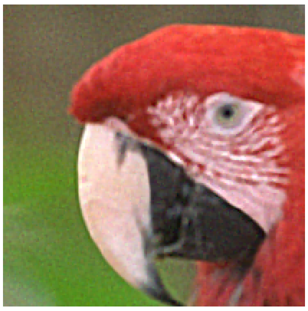

Low-frequency TV regularization + warping, PSNR=27.98

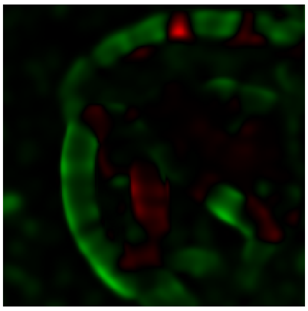

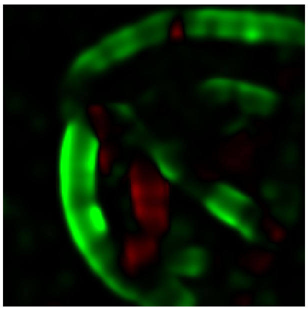

SSIM difference after image warping.
Green areas corresponds to the improvement of SSIM.
Red areas corresponds to SSIM degradation.

Fig. 7: Image post-processing by grid warping algorithm.

VI. Conclusion

The proposed generalization of the grid warping method inherits all the main advantages of the method [10], [11]. Its use as a post-processing step enables to enhance the results of existing image deblurring methods practically in all cases. No artifacts like ringing effect or noise amplification arise.

At the same time, in this work, we have shown the effectiveness of this approach for different blur kernels corresponding to real optic blur and suggested more effective single-parameter displacement function. This function is suitable for all considered blur kernels.

The work was supported by Russian Science Foundation grant 17-11-01279.

References

[1] J. Oliveira, J. M. Bioucas-Dia, and M. Figueiredo, "Adaptive total variation image deblurring: A majorization-minimization approach," *Signal Process.*, vol. 89, pp. 1683–1693, 2009.

[2] M. Almeida and M. Figueiredo, "Parameter estimation for blind and non-blind deblurring using residual whiteness measures," *IEEE Trans. Image Processing*, vol. 22, pp. 2751–2763, 2013.

[3] S. D. Babacan, R. Molina, and A. K. Katsaggelos, "Variational bayesian blind deconvolution using a total variation prior," *IEEE Trans. Image Process.*, vol. 18, pp. 12–26, 2009.

[4] J. Schavemaker, M. Reinders, J. Gerbrands, and E. Backer, "Image sharpening by morphological filtering," *Pattern Recognition*, vol. 33, no. 6, pp. 997–1012, 2000.

[5] S. Osher and L. I. Rudin, "Feature-oriented image enhancement using shock filters," *SIAM Journal on Numerical Analysis*, vol. 27, no. 4, pp. 919–940, 1999.

[6] G. Gilboa, N. A. Sochen, and Y. Y. Zeevi, "Regularized shock filters and complex diffusion," *Lecture Notes in Computer Science*, vol. 2350, pp. 399–413, 2002.

[7] J. Weickert, "Coherence-enhancing shock filters," *Lecture Notes in Computer Science*, vol. 2781, pp. 1–8, 2003.

[8] N. Arad and C. Gotsman, "Enhancement by image-dependent warping," *IEEE Trans. Image Proc.*, vol. 8, pp. 1063–1074, 1999.

[9] J. Prades-Nebot et al., "Image enhancement using warping technique," *IEEE Electronics Letters*, vol. 39, pp. 32–33, 2003.

[10] A. Krylov, A. Nasonova, and A. Nasonov, "Image warping as an image enhancement post-processing tool," *OGRW2014*, pp. 132–135, 2015.

[11] A. Nasonova and A. Krylov, "Deblurred images post-processing by Poisson warping," *IEEE Signal Processing Letters*, vol. 22, no. 4, pp. 417–420, 2015.

[12] M. Born and E. Wolf, "Principles of optics, cambridge university press," *New York*, p. 704, 1999.

[13] J. D. Simpkins, "Modeling and estimation of spatially-varying point-spread functions due to lens aberrations and defocus," Ph.D. dissertation, University of Notre Dame, 2011.

[14] J. Simpkins and R. L. Stevenson, "Parameterized modeling of spatially varying optical blur," *Journal of Electronic Imaging*, vol. 23, no. 1, pp. 013 005–013 005, 2014.

[15] J. Canny, "A computational approach to edge detection," *IEEE Trans. Pattern Analysis and Machine Intelligence*, vol. 8, pp. 679–698, 1986.

[16] N. Ponomarenko, L. Jin, O. Ieremeiev, V. Lukin, K. Egiazarian, J. Astola, B. Vozel, K. Chehdi, M. Carli, F. Battisti, and C.-C. J. Kuo, "Image database TID2013: Peculiarities, results and perspectives," *Signal Processing: Image Communication*, vol. 30, pp. 57–77, 2015.

[17] A. S. Krylov and A. V. Nasonov, "Adaptive image deblurring with ringing control," *Fifth International Conference on Image and Graphics (ICIG '09)*, pp. 72–75, 2009.

[18] J. G. Nagy, K. Palmer, and L. Perrone, "Iterative methods for image deblurring: A matlab object-oriented approach," *Numerical Algorithms*, vol. 36, no. 1, pp. 73–93, 2004.

[19] A. D. Gusev, A. V. Nasonov, and A. S. Krylov, "Parallel implementation of image sharpening method using grid warping," *Proceedings of the 26th International Conference on Computer Graphics and Vision GraphiCon'2016*, pp. 294–297, 2016.